Workshop on Robot Motion Planning:
Online, Reactive, and in Real-time
2012 IEEE/RSJ International Conference on
Intelligent Robots and Systems, IROS 2012
Vilamoura, Algarve, Portugal, October 7-12, 2012

Third Order System for the Generation of Minimum-Time Trajectories with Asymmetric Bounds on Velocity, Acceleration, and Jerk

Corrado Guarino Lo Bianco and Fabio Ghilardelli

***Abstract*— Reference signals used to drive feedback control loops are often evaluated on-the-fly on the basis of the systems operating conditions. As a consequence, it is very difficult to guarantee a priori properties like continuity or the existence of bounds on the signal dynamics and, therefore, control systems performances could deteriorate. Improved answers can be obtained if input signals are properly smoothed. The paper proposes a possible filtering system which output mimics at best any given input signal, compatibly with some smoothness requirements. In particular, generated signals are continuous up to the second time derivative and their first three time derivatives are constrained between assigned bounds. Differently from analogous solutions proposed in the past, it also handles asymmetric bounds.**

I. Introduction

The behavior of control systems is affected by the characteristics of their input signals. It is well known that, generally, system performances improve when smooth inputs are used. For this reason, when possible, references which are continuous up to the nth time derivative are adopted. Furthermore, system electro-mechanic limitations often impose bounds on the maximum allowable values of such derivatives: Tracking is lost every time bounds are violated. For these reasons reference signals that admit bounded first, second and third time derivatives are commonly used in industrial applications. Unfortunately, in many practical cases, driving signals derive from external control loops or depend on events that cannot be predicted in advance. In all these cases, smoothness cannot be guaranteed a priori and, conversely, discontinuities could easily appear. In order to avoid possible problems, rough signals are typically filtered by means of real-time planning systems, that replace them with trajectories that are characterized by the required degrees of smoothness.

Several online planners have been proposed in the literature, all of them characterized by minimum-time transients. They can be divided into two main families. In the first family, trajectories are planned by means of appropriate decision trees. In [1], in a robotic context and for continuous time frameworks, step reference signals were interpolated by means of trajectories characterized by bounded velocities, accelerations and jerks. The study was continued, for a multidimensional problem, in [2] by considering variable reference signals by fulfilling given constraints on velocities and accelerations. In [3], still for a multidimensional case, optimal online trajectories were generated for step reference signals by also managing constraints on the maximum jerk. The discrete-time solution recently devised in [4] extends previous results by also admitting generic reference signals. In the same paper an useful classification for the online trajectory planners is proposed.

In the second family, trajectories are obtained by means of dynamic filters. Such filters are constituted by a chain of integrators that are driven with variable structure sliding-mode controllers. They are able to manage generic reference signals, while output signals are still characterized by minimum-time behaviors. Early works on this approach appeared in [5], [6] and in [7], [8] respectively for continuous and discrete-time frameworks. Given solutions were based on second order filters that can guarantee the fulfillment of given bounds on the velocity and the acceleration signals. Recently, in [9], a chattering suppression method has been proposed in order to use a continuous filter within a discrete-time environment. A third-order continuous-time solution, also managing bounds on the jerk, was proposed in [10], while in [11] a dicrete-time implementation that only considers jerk bounds was synthesized. Such solution has been recently improved in [12] in order to simultaneously handle velocity, acceleration and jerk limits.

Above mentioned approaches only consider symmetric bounds. However, it is possible to cite applications, like, e.g., those proposed in [13], [14], that intrinsically admit asymmetric limits. For this reason, second-order filtering schemes, that are able to handle asymmetric constraints on the velocity and the acceleration, were proposed in [15], [14], [16]. Recently, an application that also requires the imposition of asymmetric bounds on jerk has been proposed in [17].

The new discrete-time third-order filter devised in this paper is able to generate trajectories that fulfill such requirement. Moreover, like its predecessors, it is able to manage generic reference signals, its transients are minimum-time and, finally, bounds on velocity, acceleration, and jerk can be changed in real time.

The paper is organized as follows. In §II the problem is formulated and solved by means of a novel third-order discrete-time filter. Convergence properties of the filter are analyzed in §III and in §IV. A test case is proposed in §V, while §VI reports some final conclusions.

II. The optimal trajectory scaling problem and the discrete-time filter

In the following, subscript $i \in \mathbb{Z}$ indicates sampled variables acquired at time $t = iT$, where T is the system sampling

This work was partially supported by the Ateneo Italo Tedesco in the framework of a Vigoni project.

The authors are with the Dip. di Ing. dell'Informazione, University of Parma, Italy, email: {guarino,fghilardelli}@ce.unipr.it

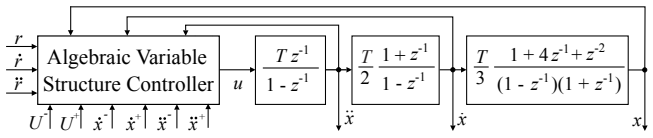

Fig. 1. The discrete-time system which solves *Problem 1*. The system is composed by a dynamic chain based on three integrators and an algebraic variable structure controller.

time. Let us consider the following problem:

Problem 1: Design a nonlinear discrete-time filter whose output x_i tracks at best a given reference signal r_i which is known together with its first and second time derivatives, while $\dddot{r}_i = 0$. The filter must guarantee that first, second, and third time derivatives of x_i are bounded between given asymmetric limits, i.e.,

$$\dot{x}^- \le \dot{x}_i \le \dot{x}^+, \quad \ddot{x}^- \le \ddot{x}_i \le \ddot{x}^+, \quad U^- \le \dddot{x}_i \le U^+ . \tag{1}$$

The bounds must be freely assignable and could be time-varying: They could also change during transients. If (1) are not satisfied, for example due to the filter initial conditions or to a sudden bounds change, $\dddot{x}$ must be forced in a single step within the given limits, while $\dot{x}$ and $\ddot{x}$ must reach the assigned bounds in minimum time. If a discontinuous signal r_i is applied, or r_i admits unfeasible time derivatives, its tracking is voluntarily lost. It is achieved again, still in minimum time, if r_i newly becomes feasible. In general, every time a feasible input signal r_i is applied to the filter, tracking condition $x_i = r_i$ must be obtained in minimum time and, compatibly with (1), without overshoot.

Practically, given any reference signal r_i, filter output x_i must track it at best compatibly with the constraints. According to the definition of *Problem 1*, feasibility is prior to optimality, thus r_i is voluntarily lost any time it becomes unfeasible. The problem is clearly similar to that considered in [12], but, as a novelty, the jerk constraint is supposed to be asymmetric. This apparently small improvement, that is essential in applications like that proposed in [17], has required a complete redefinition of the filter control laws. Practically, while the structure of the discrete-time filter, as shown in Fig. 1, is the same considered in [12], i.e., it is made of a chain of three integrators driven by an Algebraic Variable Structure Controller (AVSC), the AVSC equations have been completely redefined in order to fulfill the new requirements. The system dynamics is only due to the integrators' chain and can also be represented in the following state-space form

$$\mathbf{x}_{i+1} = \mathbf{A}\,\mathbf{x}_i + \mathbf{b}\,u_i , \tag{2}$$

where $\mathbf{x}_i := [x_i\ \dot{x}_i\ \ddot{x}_i]^T$ is the system state and

$$\mathbf{A} = \begin{bmatrix} 1 & T & \frac{T^2}{2} \\ 0 & 1 & T \\ 0 & 0 & 1 \end{bmatrix}, \quad \mathbf{b} = \begin{bmatrix} \frac{T^3}{6} \\ \frac{T^2}{2} \\ T \end{bmatrix} . \tag{3}$$

Reference signal r_i is evaluated as follows

$$\mathbf{r}_{i+1} := \mathbf{A}\,\mathbf{r}_i , \tag{4}$$

where $\mathbf{r}_i := [r_i\ \dot{r}_i\ \ddot{r}_i]^T$. A step, a ramp or a parabola are generated depending on the initial values chosen for $\dot{r}_i$ and $\ddot{r}_i$. According to the hypothesis, $\dddot{r}_i = 0$.

In order to formulate the control law for the AVSC, let us first consider the following change of coordinates $y_i := x_i - r_i$, $\dot{y}_i := \dot{x}_i - \dot{r}_i$, $\ddot{y}_i := \ddot{x}_i - \ddot{r}_i$, which places the system origin on the trajectory to be tracked. Due to (4), system (2) becomes

$$\mathbf{y}_{i+1} = \mathbf{A}\,\mathbf{y}_i + \mathbf{b}\,u_i , \tag{5}$$

where $\mathbf{A}$ and $\mathbf{b}$ coincide with (3), while $\mathbf{y}_i := [y_i\ \dot{y}_i\ \ddot{y}_i]^T$.

A further change of coordinates is required to eliminate sampling time T from matrices $\mathbf{A}$ and $\mathbf{b}$. Because of the asymmetry of the jerk constraint, required transformation $\mathbf{y}_i = \mathbf{W}\,\mathbf{z}_i$ differs from the one proposed in [12]. Indeed, the transformation matrix, that is defined as following

$$\mathbf{W} := \begin{bmatrix} T^3 & -T^3 & \frac{T^3}{6} \\ 0 & T^2 & -\frac{T^2}{2} \\ 0 & 0 & T \end{bmatrix} , \tag{6}$$

does not depend on the jerk bounds. System (5) becomes

$$\mathbf{z}_{i+1} = \mathbf{A}_d\,\mathbf{z}_i + \mathbf{b}_d\,u_i , \tag{7}$$

where $\mathbf{z}_i := [z_{1,i}\ z_{2,i}\ z_{3,i}]^T$ and

$$\mathbf{A}_d = \begin{bmatrix} 1 & 1 & 1 \\ 0 & 1 & 1 \\ 0 & 0 & 1 \end{bmatrix}, \quad \mathbf{b}_d = \begin{bmatrix} 1 \\ 1 \\ 1 \end{bmatrix} . \tag{8}$$

Matrix $\mathbf{W}$ is non singular, so that the inverse transformation $\mathbf{z}_i = \mathbf{W}^{-1}\mathbf{y}_i$ exists with

$$\mathbf{W}^{-1} = \begin{bmatrix} \frac{1}{T^3} & \frac{1}{T^2} & \frac{1}{3T} \\ 0 & \frac{1}{T^2} & \frac{1}{2T} \\ 0 & 0 & \frac{1}{T} \end{bmatrix} . \tag{9}$$

The following AVSC solves *Problem 1* (in the following, subscript i has been dropped for conciseness):

$$z_2^+ := \frac{\dot{x}^+ - \dot{r}}{T^2} - \frac{\ddot{r}}{2T} , \tag{10}$$

$$z_2^- := \frac{\dot{x}^- - \dot{r}}{T^2} - \frac{\ddot{r}}{2T} , \tag{11}$$

$$z_3^+ := \frac{\ddot{x}^+}{T} , \tag{12}$$

$$z_3^- := \frac{\ddot{x}^-}{T} , \tag{13}$$

$$\overline{z}_2^+ := -\left\lceil -\frac{z_3^+}{U^-} \right\rceil \left[z_3^+ + \frac{U^-}{2}\left(\left\lceil -\frac{z_3^+}{U^-} \right\rceil - 1 \right) \right] , \tag{14}$$

$$\overline{z}_2^- := -\left\lceil -\frac{z_3^-}{U^+} \right\rceil \left[z_3^- + \frac{U^+}{2}\left(\left\lceil -\frac{z_3^-}{U^+} \right\rceil - 1 \right) \right] , \tag{15}$$

$$d_1 := z_2 - z_2^+ , \tag{16}$$

$$d_2 := z_2 - z_2^- , \tag{17}$$

for n=1,2:

$$\gamma_n := \begin{cases} \overline{z}_2^+ & \text{if } d_n < \overline{z}_2^+ \\ d_n & \text{if } \overline{z}_2^+ \le d_n \le \overline{z}_2^- \\ \overline{z}_2^- & \text{if } d_n > \overline{z}_2^- \end{cases} , \tag{18}$$

$$\kappa_n := \begin{cases} U^- & \text{if } d_n \le 0 \\ U^+ & \text{if } d_n > 0 \end{cases} , \tag{19}$$

$$m_n := \left\lfloor \frac{1}{2} + \sqrt{\frac{1}{4} + 2\left|\frac{\gamma_n}{\kappa_n}\right|} \right\rfloor , \tag{20}$$

$$\sigma_n := -\frac{\gamma_n}{m_n} - \frac{m_n - 1}{2}\kappa_n - \frac{\ddot{r}}{T} , \tag{21}$$

end for

$$[\alpha\ \beta] := \begin{cases} [U^-\ U^+] & \text{if } \eta > 0 \\ [U^+\ U^-] & \text{if } \eta \leq 0 \end{cases} , \tag{22}$$

$$\begin{aligned} \sigma_3 \quad := \quad & -\frac{2}{h(h+k)}z_1 - \frac{2h+k-1}{h(h+k)}z_2 - \frac{k(1-k^2)}{6h(h+k)}\alpha \\ & -\frac{2h^3-3h^2+h+3h^2k-3hk}{6h(h+k)}\beta , \end{aligned} \tag{23}$$

$$\sigma := \begin{cases} \sigma_1 & \text{if} \quad \sigma_1 < \sigma_3 \\ \sigma_3 & \text{if} \quad \sigma_2 \leq \sigma_3 \leq \sigma_1 \\ \sigma_2 & \text{if} \quad \sigma_3 < \sigma_2 \end{cases} , \tag{24}$$

$$\delta := z_3 - \sigma , \tag{25}$$

$$u := \begin{cases} -U^- \text{sat}\left(\dfrac{\delta}{U^-}\right) & \text{if} \quad \delta \geq 0 \\ -U^+ \text{sat}\left(\dfrac{\delta}{U^+}\right) & \text{if} \quad \delta < 0 \end{cases} , \tag{26}$$

where z_1, z_2 and z_3 are the three components of $\mathbf{z}$, while integers h, k, and η are functions of z_1 and z_2. Details on the definition of h, k, and η can be found [11]. The two operators $\lfloor\cdot\rfloor$ and $\lceil\cdot\rceil$ respectively evaluate the floor and the ceil of a real number. Function $\text{sat}(\cdot)$ saturates its argument to ± 1.

The AVSC is designed by means of sliding mode techniques in order to robustly drive the system state toward the origin, i.e., toward $\mathbf{z} = 0$, compatibly with the constraints. This as well implies that $\mathbf{y}$ is driven toward the origin, which, in turn, means that output x tracks r. The AVSC achieves this result by switching, according to (24), between three different Sliding Surfaces (SS), namely σ_1, σ_2, and σ_3, each of them surrounded by an appropriate Boundary Layer (BL). The three SSs cover the same roles of those proposed in [12]: σ_3 drives the system toward the origin in minimum time and by simultaneously fulfilling the jerk constraint, while σ_1 and σ_2 are used to satisfy the velocity and acceleration bounds. The switching criteria is the same implemented in [12], so that the reader can refer to that work for details concerning the underlying mechanisms. Since feasibility represents the prior target, σ_1 and σ_2 are primarily selected in order to accomplish this requirement in minimum time, but, as soon as feasibility does no more represent an issue, σ_3 is used in order to reach the origin in minimum time. Similarities with the filter proposed in [12] end here, since the three surfaces, due to the constraints asymmetry, have been completely redesigned.

In the next sections the filter is analyzed in detail. In particular, in §III the characteristics of σ_3 are investigated in order to prove that such surface robustly leads the system toward the origin in minimum time by simultaneously fulfilling the constraint on the maximum jerk. Then, §IV will show that, by means of the two additional surfaces σ_1 and σ_2, it is possible to robustly guarantee the convergence of the state toward an area that is feasible with respect to the velocity and the acceleration constraints.

III. The convergence properties of σ_3

In order to prove that σ_3 drives the system in minimum time toward the origin, it is first necessary to identify the set of points in the $\mathbf{z}$-space from which the origin itself can be reached in minimum time compatibly with the constraint on the maximum jerk. Such points can be found by applying the maximum admissible values of command signal u, i.e., $u = U^+$ or $u = U^-$ and by backward integrating system (7). Let us define an additional parameter $\eta = \pm 1$: If $\eta = 1$ then command signal $u = U^-$ is initially used, while, viceversa, if $\eta = -1$ then $u = U^+$. According to this procedure, the following set of points is obtained

$$\mathbf{p}(k,\eta) = \begin{bmatrix} -\frac{1}{6}k\left(k^2-3k+2\right)\alpha \\ \frac{1}{2}k\left(k-1\right)\alpha \\ -k\alpha \end{bmatrix} , \tag{27}$$

where α depends on η and it is evaluated according to (22), while $k \in \mathbb{Z}$ indicates the number of back integrations occurred.

Remark 1: Given any point defined according to (27), it is immediately possible to know the number of steps required to converge toward the origin, e.g., from point $\mathbf{p}(k,\eta)$ the origin is reached in minimum time after k sampling times. Points $\mathbf{p}(k,\eta)$ can be used as initial conditions for a further backward integration process. If a generic point $\mathbf{p}(k,1)$, has been reached by using $u = U^-$, the new backward process will adopts $u = U^+$. Similarly, command signal $u = U^-$ is used for points $\mathbf{p}(k,-1)$. In this way, the following new set of points $\mathbf{p}(h,k,\eta)$ is found

$$\mathbf{p}(h,k,\eta) = \begin{bmatrix} -\left[\frac{k(k-1)(k-2)}{6} + \frac{hk(h+k-2)}{2}\right]\alpha - \frac{h(h-1)(h-2)}{6}\beta \\ \left[\frac{k(k-1)}{2} + hk\right]\alpha + \frac{h(h-1)}{2}\beta \\ -k\alpha - h\beta \end{bmatrix} \tag{28}$$

where α and β, according to (22), depend on η, while k and h indicate the number of steps occurred, respectively, during the first and the second backward integration phases.

Remark 2: Given any point defined according to (28), it is immediately possible to know the number of steps required to converge toward the origin, more precisely h steps are necessary to reach points $\mathbf{p}(k,\eta)$ and, then, further k steps are required to converge to the origin. Practically, the origin is reached in minimum time with a bang-bang control.

To simplify the notation, let us define $\mathbf{p}^-_{h,k} := \mathbf{p}(h,k,-1)$ and $\mathbf{p}^+_{h,k} := \mathbf{p}(h,k,1)$. Points $\mathbf{p}^-_{h,k}$ and $\mathbf{p}^+_{h,k}$, as shown in Fig. 2, completely cover the (z_1,z_2)-space, that is partitioned into two sectors depending on η.

This premises are instrumental to demonstrate that the control law defined through equations (22), (23), (26) with

$$\delta = z_3 - \sigma_3 , \tag{29}$$

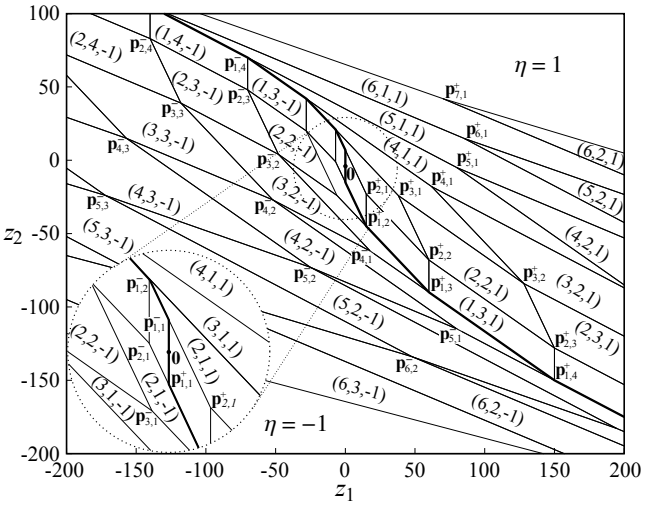

Fig. 2. Boxes (h,k,η) and points $\mathbf{p}(h,k,\eta)$ projected on the (z_1,z_2)-space.

is time-optimal and fulfills the jerk constraint. In particular, this second characteristic is immediately evident from (26): In any case $u \in [U^-, U^+]$.

As early anticipated, an AVSC, that is based on sliding mode techniques, is used to this purpose. Equation (22), depending on the current value of η, switches between two different SSs. Equation (23) expresses both of them: Because of (22), they change in function of η. Finally, (26) wraps the SS within an appropriate BL. As shown in Fig. 3, there exists a direct relationship between the SSs and points $\mathbf{p}^+_{h,k}$: Equations (22), (23), (26), and (29) associate to each point $\mathbf{p}^+_{h,k}$ a box, that is identified in the following as $(h,k,1)$, which upper/lower surfaces coincide with the upper/lower BLs of the SS.

To our purposes, it is essential to prove that the adopted control law is time-optimal. Evidently, Fig. 2 shows that σ_3 covers the whole (z_1,z_2)-space, so that, by applying $u = U^+$, the BL is certainly reached in minimum time from points placed below the SS. The same happens for points placed above the SS if command $u = U^-$ is used. In the following it will be proved that once the state enters inside any generic box (h,k,η), it slides toward the origin in minimum time. In particular, if the starting point is $\mathbf{p}(h,k,\eta)$ the convergence is achieved, as expected, in $h+k$ steps, while for any other point lying in (h,k,η) the origin is reached in $h+k+1$ steps.

Property 1: Consider system (7) and an initial state located inside box (h,k,η), with $h,k > 1$. By applying control law (22), (23), (26), and (29) the system evolves, in a single step, to a new state located in box $(h-1,k,\eta)$.

Proof: Let us assume that at step i system state $\mathbf{z}_i$ lies inside box (h,k,η). By defining the following three independent vectors

$$\bar{\mathbf{e}}_r(h,k,\eta) := \begin{bmatrix} -\frac{1}{2}\left[k(k-1)+h(h-1)+2hk\right]\alpha \\ (h+k)\,\alpha \\ -\alpha \end{bmatrix}, \quad (30)$$

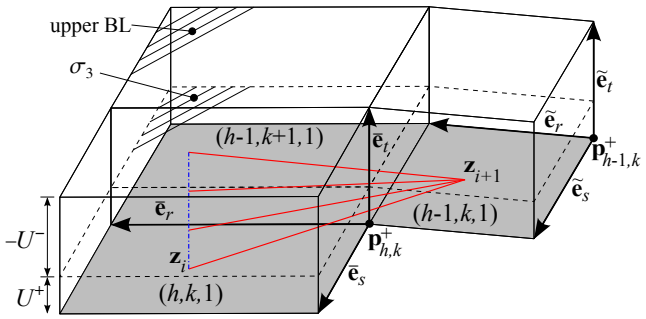

Fig. 3. Single step evolution starting from box $(h,k,1)$

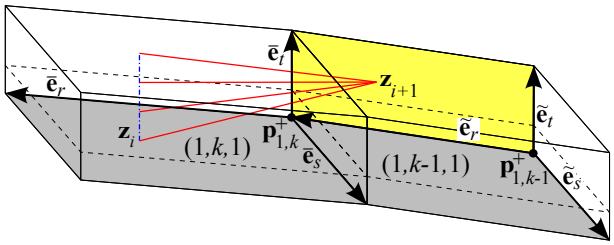

Fig. 4. Single step evolution starting from box $(1,k,1)$.

$$\bar{\mathbf{e}}_s(h,k,\eta) := \begin{bmatrix} \frac{1}{2}h(h-1) \\ -h \\ 1 \end{bmatrix} (\alpha-\beta), \quad (31)$$

$$\bar{\mathbf{e}}_t(h,k,\eta) := \begin{bmatrix} 0 \\ 0 \\ \beta-\alpha \end{bmatrix}, \quad (32)$$

which position is shown in Fig. 3 for $\eta = 1$, it is possible to describe $\mathbf{z}_i$ as follows

$$\mathbf{z}_i = \mathbf{p}(h,k,\eta) + \lambda\,\bar{\mathbf{e}}_r(h,k,\eta) + \mu\,\bar{\mathbf{e}}_s(h,k,\eta) + \nu\,\bar{\mathbf{e}}_t(h,k,\eta), \quad (33)$$

with $\lambda,\mu,\nu \in [0,1)$, $h,k > 1$ and where $\mathbf{p}(h,k,\eta)$ is defined according to (28).

For $\mathbf{z} = \mathbf{z}_i$ the control law returns $u = \nu\,\alpha + (1-\nu)\,\beta$ so that the state of system (7), at step $i+1$, evolves to

$$\mathbf{z}_{i+1} = \mathbf{p}(h-1,k,\eta) + \lambda\,\tilde{\mathbf{e}}_r + \mu\,\tilde{\mathbf{e}}_s,$$

where $\tilde{\mathbf{e}}_r(h,k,\eta) = \bar{\mathbf{e}}_r(h,k,\eta)|_{h=h-1}$, and $\tilde{\mathbf{e}}_s(h,k,\eta) = \bar{\mathbf{e}}_s(h,k,\eta)|_{h=h-1}$. Point $\mathbf{z}_{i+1}$ is evidently located inside box $(h-1,k,\eta)$ and, more precisely, it lies on its lower BL if $\eta = 1$, or on its upper BL if $\eta = -1$. It is worth noticing that points $\mathbf{z}_i$, which admit the same values of λ and μ are projected in the same point $\mathbf{z}_{i+1}$, independently from ν. ■

Evidently, since *Property 1* applies for any generic point of box (h,k,η) with $h,k > 1$, the system state reaches box $(1,k,\eta)$ after $h-1$ steps.

Property 2: Consider system (7) and an initial state located inside box $(1,k,\eta)$, with $k > 1$. By applying control law (22), (23), (26), and (29) the system evolves, in a single step, to a new state located in box $(1,k-1,\eta)$.

Proof: Assume that at step i the system state $\mathbf{z}_i$ lies inside box $(1,k,\eta)$, so that it can be described by means of (33) by assuming $\lambda,\mu,\nu \in [0,1)$, $h = 1$, $k > 1$. The control

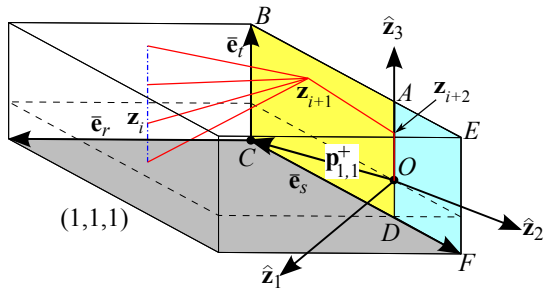

Fig. 5. Final evolution: If the system state enters into box $(1,1,1)$, it is forced toward the origin within three steps. Surface ABCD is contained into the plane individuated by unit vectors $\hat{\mathbf{z}}_2$ and $\hat{\mathbf{z}}_3$.

law still returns $u = \nu\,\alpha + (1-\nu)\,\beta$ and, consequently, the state evolves as follows

$$\mathbf{z}_{i+1} = \mathbf{p}(1,k-1,\eta) + \lambda\,\tilde{\mathbf{e}}_r + (1-\mu)\,\tilde{\mathbf{e}}_t,$$

with $\tilde{\mathbf{e}}_r(1,k,\eta) = \bar{\mathbf{e}}_r(1,k,\eta)|_{k=k-1}$, and $\tilde{\mathbf{e}}_t(1,k,\eta) = \bar{\mathbf{e}}_t(1,k,\eta)|_{k=k-1}$. State $\mathbf{z}_{i+1}$ is evidently located inside box $(1,k-1,\eta)$ and, more precisely, since component $\tilde{\mathbf{e}}_s$ is missing, it lies on a lateral face of the box. Again, as shown in Fig.4, points $\mathbf{z}_i$ that admit the same values of λ and μ are plotted in the same point $\mathbf{z}_{i+1}$ independently from ν. ■

According to *Properties 1* and *2*, starting from any generic box (h,k,η) with $h,k>1$, the system state evolves into box $(1,1,\eta)$ after $h+k-2$ steps. The final convergence toward the origin is analyzed in the following property:

Property 3: Consider system (7) and an initial state located inside box $(1,1,\eta)$. By means of control law (22), (23), (26), and (29) the state reaches the origin with a maximum of three transitions.

Proof: Assume that at step i the system state $\mathbf{z}_i$ is located inside box $(1,1,\eta)$, so that it can be described by means of (33) by assuming $\lambda,\mu,\nu \in [0,1)$, $h,k=1$. The command law returns $u = \nu\,\alpha + (1-\nu)\,\beta$ and the state evolves, in a single step, as follows

$$\mathbf{z}_{i+1} = \mathbf{p}(1,1,\eta) + \delta\,\bar{\mathbf{e}}_s(1,1,\eta) + \varepsilon\,\bar{\mathbf{e}}_t(1,1,\eta),$$

where $\delta \in \left[0, -\frac{\alpha}{\beta-\alpha}\right]$ and $\varepsilon \in [0,1]$. It is easy to verify that, when $\eta = 1$, point $\mathbf{z}_{i+1}$ is located on surface *ABCD* of Fig. 5, while when $\eta = -1$ it lies on surface *AEFD*.

If a further step is executed from $\mathbf{z}_{i+1}$ the command signal becomes $u = \varepsilon\,\alpha + (1-\varepsilon)\,\beta$ and the state is forced to point $\mathbf{z}_{i+2} := [0\ 0\ (\delta-1)\,\alpha - \delta\,\beta]^T$. Bearing in mind the definition of δ, it is evident that, if $\mathbf{z}_{i+1}$ lies on *ABCD* ($\eta = 1$), then $\mathbf{z}_{i+2}$ is located on segment *OA*, while, if $\mathbf{z}_{i+1}$ lies on *AEFD* ($\eta = -1$), then $\mathbf{z}_{i+2}$ is located on *OD*.

Finally, for any point $\mathbf{z}_{i+2}$ located on segment *AD*, still with command signal $u = \varepsilon\,\alpha + (1-\varepsilon)\,\beta$, the state is forced to the origin in a single step. ■

In conclusion, if the initial state is located inside box (h,k,η), it evolves toward the origin in no more than $h+k+1$ steps. It is possible to verify that if the initial state is equal to $\mathbf{p}(h,k,\eta)$ then $h+h-2$ step are required to reach point $\mathbf{p}(1,1,\eta)$, while only two more steps are required to reach the origin: Convergence is achieved in $h+k$ steps, thus confirming the solution optimality.

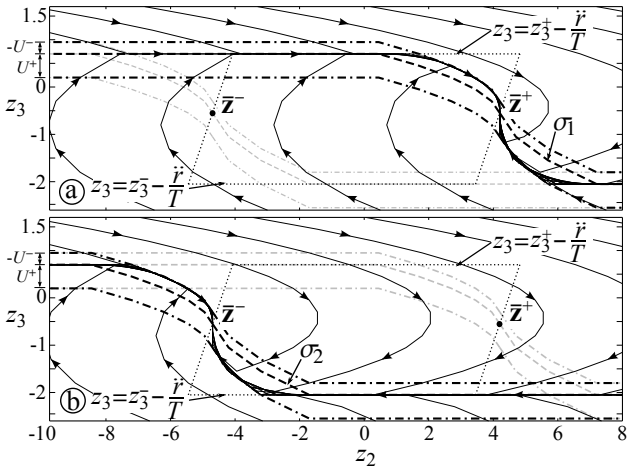

Fig. 6. System trajectories in the (z_2,z_3)-space obtained by assuming: a) $\sigma = \sigma_1$ and b) $\sigma = \sigma_2$. SSs σ_1 and σ_2 are indicated by means of dashed lines and are surrounded by their BLs (dash dotted lines). The dotted quadrangle contours the feasible area.

IV. The Convergence Properties of σ_1 and σ_2

Surfaces σ_1 and σ_2 are designed to force the system, in minimum time, within a zone where the velocity and the acceleration constraints are fulfilled. One of the two surfaces is chosen by means of (24) every time σ_3 should drive the state outside the feasible area. Such area, defined in the $(\dot{x},\ddot{x})$-space by means of a rectangle delimited by lines $\dot{x} = \dot{x}^+$, $\dot{x} = \dot{x}^-$, $\ddot{x} = \ddot{x}^+$, and $\ddot{x} = \ddot{x}^-$, can be converted into an equivalent area in the (z_2,z_3)-space. More precisely, the velocity bounds, i.e., $\dot{x} = \dot{x}^+$ and $\dot{x} = \dot{x}^-$, are respectively converted into the following limits $z_3 = 2\left(z_2 - z_2^+ + \frac{\ddot{r}}{2T}\right)$, $z_3 = 2\left(z_2 - z_2^- + \frac{\ddot{r}}{2T}\right)$, while the acceleration bounds, i.e., $\ddot{x} = \ddot{x}^+$ and $\ddot{x} = \ddot{x}^-$, become $z_3 = z_3^+ - \frac{\ddot{r}}{T}$, and $z_3 = z_3^- - \frac{\ddot{r}}{T}$. Dotted lines of Fig. 6 highlight the converted feasible area. Evidently, it is independent from z_1, and, for this reason, the following discussion will only focus on the state evolution in the (z_2,z_3)-subspace. Fig. 6 also shows σ_1 and σ_2 with the corresponding BLs and the system trajectories: The maximum command signals, i.e., $u = U^+$ or $u = U^-$, are used when the state is outside the BLs, so that the area within the two accelerations limits, i.e., within $z_3 = z_3^+ - \frac{\ddot{r}}{T}$ and $z_3 = z_3^- - \frac{\ddot{r}}{T}$, is certainly reached in minimum time. Then, the state is driven, depending on which of the two SS is used, toward $\bar{\mathbf{z}}^+$ or toward $\bar{\mathbf{z}}^-$. In any case, the desired result is achieved, since both points are evidently feasible with respect to the velocity and the acceleration constraints. States $\bar{\mathbf{z}}^+$ and $\bar{\mathbf{z}}^-$ are obtained by transforming points $(\dot{x}^+,0)$ and $(\dot{x}^-,0)$ of the $(\dot{x},\ddot{x})$-space. Practically, when σ_1 (or σ_2) is chosen, the system is forced in minimum time in $(\dot{x}^+,0)$ [or in $(\dot{x}^-,0)$]: With arguments analogous to those reported in [12], it is possible to prove that the system state, when it is locked in one of those two states, moves with zero acceleration and at the maximum speed toward σ_3. When such surface is reached, $\bar{\mathbf{z}}^+$ (or $\bar{\mathbf{z}}^-$) is abandoned and the system can finally converge to the origin with a feasible trajectory.

Surfaces σ_1 and σ_2 have been obtained by modifying the analogous surface proposed in [16]. Indeed, bearing in mind

(7) and (8), the system evolution in the $(\dot{x},\ddot{x})$-space can be expressed by the following state equation

$$\begin{bmatrix} z_{2,i+1} \\ z_{3,i+1} \end{bmatrix} = \begin{bmatrix} 1 & 1 \\ 0 & 1 \end{bmatrix} \begin{bmatrix} z_{2,i} \\ z_{3,i} \end{bmatrix} + \begin{bmatrix} 1 \\ 1 \end{bmatrix} u_i, \qquad (34)$$

i.e., the model is the same of the system already considered in [16], but the role of the pair z_1 and z_2 is now played by z_2 and z_3. Thus, by using the same control law proposed in that paper, the same convergence properties are evidently maintained: The sole difference that has been introduced is that σ_1 and σ_2 are modified with respect to the original SS, so that the state does not converge to the origin but, conversely it converges to $\overline{\mathbf{z}}^+$ or to $\overline{\mathbf{z}}^-$.

V. A TEST CASE

In the test case of Fig. 7 the filter handles a discontinuous signal made of steps, ramps and parabolas. The following kinematic bounds have been initially assumed: $\dot{x}^+ = 2.5$ m s^{-1}, $\dot{x}^- = -3$ m s^{-1}, $\ddot{x}^+ = 3.5$ m s^{-2}, $\ddot{x}^- = -4.9$ m s^{-2}, $U^+ = 10$ m s^{-3}, $U^- = -15$ m s^{-3}. Fig. 7a compares the original discontinuous signal with the filter outputs: x tracks at best reference r, compatibly with the given constraints. The small undershoot, that is highlighted by the dotted circle, appears if the acceleration constraint is touched during the final transient toward r. Indeed, any time such bound is activated, the control switches to σ_1 or to σ_2, thus the state abandon σ_3 and an overshoot is produced. This problem can be eliminated by managing the acceleration constraint directly with σ_3. Studies on this topic are undergoing.

The filter bounds are changed at $t = 6.4$ s: $\dot{x}^+ = 1.5$ m s^{-1}, $\dot{x}^- = -2$ m s^{-1}, $\ddot{x}^+ = 3$ m s^{-2}, $\ddot{x}^- = -3.9$ m s^{-2}, $U^+ = 9$ m s^{-3}, $U^- = -9$ m s^{-3}. The system immediately generates trajectories that fulfill the new limits.

A new bounds change is planned in a critical situation, i.e., when the filter is in the middle of a transient toward a ramp. In particular, at $t = 12.5$ s, constraints assume the following values: $\dot{x}^+ = 1.5$ m s^{-1}, $\dot{x}^- = -1$ m s^{-1}, $\ddot{x}^+ = 5.5$ m s^{-2}, $\ddot{x}^- = -1.9$ m s^{-2}, $U^+ = 7$ m s^{-3}, $U^- = -9$ m s^{-3}. Owing to these sudden changes, constraints are instantly violated (see the dash-dotted circles in Fig. 7). As required, jerk bounds are fulfilled in a single step, while acceleration and velocity limits are satisfied in minimum time, compatibly with the jerk constraints. Thus, according to the requirements, the constraints fulfillment is considered prior with respect to the convergence toward the origin: The ramp is hanged, still in minimum time, only after the signal feasibility is guaranteed.

VI. CONCLUSIONS

The discrete-time filter proposed in the paper is able to generate, starting from rough references which continuity is not guaranteed, signals that are continuous together with their first and second time derivatives. Moreover, it is able to implicitly impose bounds on the first, the second, and the third time derivatives of the output signal. Generated transients are minimum-time. Differently from analogous filters proposed in the past, it robustly handles asymmetric constraints.

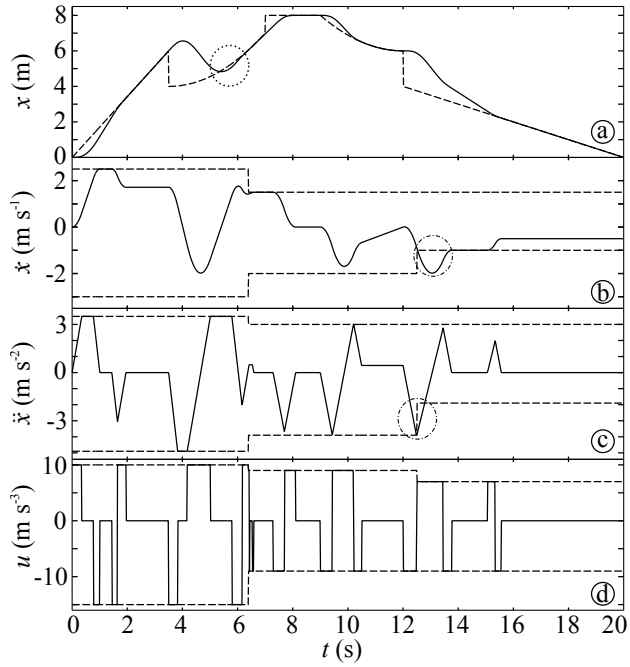

Fig. 7. The simulated test case: a) the non-smooth reference signal (dashed line) is compared with the filter output x (solid line); b) filter velocity signal $\dot{x}$ (solid line) compared with the given bounds (dashed lines) c) filter acceleration $\ddot{x}$ (solid line) compared with the given bounds (dashed lines) d) filter jerk signal $\dddot{x}$ (solid line) compared with the given bounds (dashed lines).

The proposed planner is characterized by several advantages. First of all, it has a structure that is extremely simple: The code length required for the implementation of the sliding mode controller is negligible, so that the filter can even be implemented in systems with reduced memory capabilities. Also the computational burden is particularly light: The average evaluation time detected with a PC based on an Intel Core2 Duo processor, @3GHz, and equipped with a RTAI patched operating system, is equal to 4.32e-6 s.

REFERENCES

[1] S. Liu, "An on-line reference-trajectory generator for smooth motion of impulse-controlled industrial manipulators," in *Proc. of the seventh Int. Work. on Advanced Motion Control*, 2002, pp. 365–370.

[2] R. Haschke, E. Weitnauer, and H. Ritter, "On-line planning of timeoptimal, jerk-limited trajectories," in *Proc. of the IEEE/RSJ Int. Conf. on Intelligent Robots and Systems, IROS 08*, 2008, pp. 3248–3253.

[3] X. Broquère, D. Sidobre, and I. Herrera-Aguilar, "Soft motion trajectory planner for service manipulator robot," in *Proc. of the 2008 IEEE/RSJ Int. Conf. on Intelligent Robots and Systems, IROS 08*, 2008, pp. 2808–2813.

[4] T. Kröger and F. M. Wahl, "On-Line Trajectory Generation: Basic Concepts for Instantaneous Reactions to Unforeseen Events," *IEEE Trans. on Robotics*, vol. 26, no. 1, pp. 94–111, Feb. 2010.

[5] C. Guarino Lo Bianco, A. Tonielli, and R. Zanasi, "Nonlinear trajectory generator," in *IECON96 - 22nd Annual International Conference on the IEEE Industrial Electronics Society*, Taiwan, Taipei, August 1996, pp. 195–201.

[6] R. Zanasi, A. Tonielli, and C. Guarino Lo Bianco, "Nonlinear filter for smooth trajectory generation," in *NOLCOS98 - 4th Nonlinear Control Systems Design Symp.*, vol. 1, Enschede, the Netherlands, July 1998, pp. 245–250.

[7] R. Zanasi, C. Guarino Lo Bianco, and A. Tonielli, "Nonlinear filters for the generation of smooth trajectories," *Automatica*, vol. 36, no. 3, pp. 439–448, March 2000.

[8] C. Guarino Lo Bianco and R. Zanasi, "Smooth profile generation for a tile printing machine," *IEEE Trans. on Ind. Electronics*, vol. 50, no. 3, pp. 471–477, 2003.

[9] L. Biagiotti and R. Zanasi, "Online trajectory planner with constraints on velocity, acceleration and torque," in *Proc. of the IEEE Int. Symp. on Ind. Electr., ISIE2010*, Bari, Italy, Jul. 2010, pp. 274–279.

[10] R. Zanasi and R. Morselli, "Third order trajectory generator satisfying velocity, acceleration and jerk constraints," in *Proc. of the 2002 IEEE Int. Conf. on Control Applications*, Glasgow, Scotland, UK, Sept. 2002, pp. 1165–1170.

[11] ——, "Discrete minimum time tracking problem for a chain of three integrators with bounded input," *Automatica*, vol. 39, no. 9, pp. 1643–1649, 2003.

[12] O. Gerelli and C. Guarino Lo Bianco, "A discrete-time filter for the online generation of trajectories with bounded velocity, acceleration, and jerk," in *IEEE Int. Conf. on Rob. and Autom., ICRA2010*, Anchorage, AK, May 2010, pp. 3989–3994.

[13] D. Kubus, D. Inkermann, T. Vietor, and F. M. Wahl, "Joint Actuation Based on Highly Dynamic Torque Transmission Elements – Concept and Control Approaches," in *Proc. of IEEE Int. Conf. on Rob. and Autom., ICRA 2011*, Shanghai, China, May 2011, pp. 2777–2784.

[14] C. Guarino Lo Bianco and O. Gerelli, "Trajectory scaling for a manipulator inverse dynamics control subject to generalized force derivative constraints," in *2009 IEEE/RSJ Int. Conf. on Intell. Robots and Systems, IROS 2009*, St. Louis, MO, Oct. 2009, pp. 5749–5754.

[15] O. Gerelli and C. Guarino Lo Bianco, "Real-time path-tracking control of robotic manipulators with bounded torques and torque-derivatives," in *2008 IEEE/RSJ Int. Conf. on Intelligent Robots and Systems, IROS 2008*, Nice, France, Sep. 2008, pp. 532–537.

[16] C. Guarino Lo Bianco and F. Wahl, "A novel second order filter for the real-time trajectory scaling," in *Proc. of the 2011 IEEE Int. Conf. on Robotics and Automation, ICRA 2011*, Shanghai, China, May 9–13 2011, pp. 5813–5818.

[17] C. Guarino Lo Bianco and O. Gerelli, "Online Trajectory Scaling for Manipulators Subject to High-Order Kinematic and Dynamic Constraints," *IEEE Trans. on Robotics*, vol. 27, no. 6, pp. 1144–1152, Dec. 2011.